



TITLE:

Contrast matching of an Si substrate with polymer films by anomalous dispersion at the Si

AUTHOR(S):

Okuda, Hiroshi; Takeshita, Kohki; Ochiai, Shojiro; Kitajima, Yoshinori; Sakurai, Shinichi; Ogawa, Hiroki

CITATION:

Okuda, Hiroshi ...[et al]. Contrast matching of an Si substrate with polymer films by anomalous dispersion at the Si. Journal of Applied Crystallography 2012, 45(1): 119-121

ISSUE DATE:

2012-02

URL:

<http://hdl.handle.net/2433/153285>

RIGHT:

© 2012 International Union of Crystallography

Contrast matching of an Si substrate with polymer films by anomalous dispersion at the Si *K* absorption edge

Hiroshi Okuda,^{a*} Kohki Takeshita,^b Shojiro Ochiai,^a Yoshinori Kitajima,^c Shinichi Sakurai^d and Hiroki Ogawa^e

^aDepartment of Materials Science and Engineering, Kyoto University, Japan, ^bGraduate School of Engineering, Kyoto University, Japan, ^cPhoton Factory, KEK, Japan, ^dKyoto Institute of Technology, Japan, and ^eJapan Synchrotron Radiation Research Institute, SPring-8, Japan. Correspondence e-mail: okuda@materials.mbox.media.kyoto-u.ac.jp

Anomalous dispersion at the Si *K* absorption edge has been used to control the reflection from the interface between a film and an Si substrate, which otherwise complicates the nanostructure analysis of such a film, particularly for the soft-matter case, in grazing-incidence small-angle scattering. Such a reflectionless condition has been chosen for a triblock copolymer thin film, and two-dimensional grazing-incidence small-angle scattering patterns were obtained without the effect of the reflection. The present approach is useful for analysing nanostructures without introducing complicated corrections arising from the reflection.

© 2012 International Union of Crystallography
Printed in Singapore – all rights reserved

1. Introduction

X-ray scattering under grazing incidence has been proven to be a powerful nondestructive tool for understanding nanostructures and their evolution during growth (Levine *et al.*, 1989; Babonneau *et al.*, 2000; Renaud *et al.*, 2009). In particular, this approach is used for very thin soft-matter films containing three-dimensional nanostructures prepared on a well defined substrate, such as an Si wafer, because cross-sectional imaging using microscopic approaches is often difficult for such materials (Tolan, 1999; Saldit *et al.*, 2006). However, strong reflection from the film surface and the film/substrate interface often makes it difficult to obtain detailed information about the structure of the film. Detailed analysis of such a film using grazing-incidence small-angle X-ray scattering (GISAXS) often requires taking the effects of the reflected beam into account (Sinha *et al.*, 1988; Rauscher *et al.*, 1995; Lazzari, 2002) under the distorted-wave Born approximation (DWBA). With the DWBA, a scattering intensity profile contains the form factor of a scattering object having different scattering vectors in the perpendicular direction for the same detector position, given by Lee *et al.* (2005) as

$$F(q_{\parallel}, k_{\parallel}^z, k_{\perp}^z) = T_i T_f F(q_{\parallel}, k_{\parallel}^z - k_{\perp}^z) + T_i R_f F(q_{\parallel}, -k_{\parallel}^z - k_{\perp}^z) + R_i T_f F(q_{\parallel}, k_{\parallel}^z + k_{\perp}^z) + R_i R_f F(q_{\parallel}, -k_{\parallel}^z + k_{\perp}^z), \quad (1)$$

where *T* and *R* are the Fresnel transmission and reflection coefficients, respectively, *F*(*q*_∥, *q*_⊥) is the form factor of the scattering object, *k*_∥^z and *k*_⊥^z are the *z* components of the incoming and outgoing wave vectors, respectively, and *q*_∥ is the magnitude of the in-plane scattering vector.

For polymer films having periodic structures like lamellae or rods, the correction terms from the DWBA result in extra diffraction peaks, as reported by Lee *et al.* (2005) and Busch *et al.* (2006). The analysis may become more difficult when a scattering pattern is less periodic and changes monotonically with the scattering angle. Further difficulties arise because the specular reflectivity or diffuse scattering intensities depend not only on the film microstructure,

which causes small-angle scattering, but also on the surface and interface morphology, in particular on the thickness of the films and the roughness at the film/substrate interface. A scattering pattern with such effects can be further complicated because the wave directly scattered by the incident X-rays [the first term of the right-hand side of equation (1), the so-called Born term] may or may not interfere with the scattering waves involved in the reflection at the film/substrate interface [the other three terms of the right-hand side of equation (1)]. Improving the analysis by controlling the contrast in the sample is an established method in neutron scattering techniques, utilizing isotopes such as deuterium (Ibel & Stuhmann, 1975; Stuhmann, 2007). Thin soft-matter films are generally much lighter than their substrates, and therefore strong contrast in the refractive index is inevitable with the hard X-rays that are commonly used for structure analysis. However, with a large anomalous dispersion effect at the Si *K* absorption edge, it may be expected that the real part of the refractive index of Si is even lower than that of such soft-matter films. Fig. 1(*a*) shows the real parts of the refractive indices of the film and substrate calculated from the reported anomalous dispersion term (Chantler, 1997). As shown in the figure, the real part of the refractive index of the Si substrate drops sharply at the *K* absorption edge and eventually matches that of the polymer film. Model reflectivity calculations for a polymer film having the refractive index and thickness of the present sample are shown in Fig. 1(*b*). The Kiessig fringe becomes much weaker at 1.837 keV, meaning that the reflection from the polymer/Si interface is very small, although it is not completely suppressed because of the difference in the imaginary part of the refractive index (Ishiji *et al.*, 2002). Accordingly, the strong effect of the X-ray beam reflected from the polymer/substrate interface can be avoided by choosing a photon energy very close to the absorption edge, even though the amplitude of the incoming electromagnetic field of the X-rays is still strong at the interface. It is also noted that the refractive index of the Si substrate can even be matched with water.

short communications

2. Experimental

The samples used in the present work are styrene–polystyrene–block-poly(ethylenebutylene)–block-polystyrene (SEBS) triblock copolymer films prepared by spin-casting of a toluene solution on Si substrates (Okuda *et al.*, 2011). The nominal thickness of the films was 50 nm. The film thickness and density were evaluated by ellipsometry and X-ray reflectivity measurements. The samples were annealed at 413 K for 8 h to form a micro phase-separated structure. Bulk samples with the same heat treatment exhibit microstructures in which the cores are arranged in a body-centred cubic structure. GISAXS measurements at the Si *K* absorption edge were performed at Beamline 11B of the Photon Factory, KEK, Tsukuba, Japan (Okuda *et al.*, 2009), and those with hard X-rays were performed at Beamline 03XU of Spring8, Hyogo, Japan (Masunaga *et al.*, 2011). The photon energies chosen for the resonant GISAXS measurements at the Si *K* edge were 1.770, 1.830 and 1.837 keV.

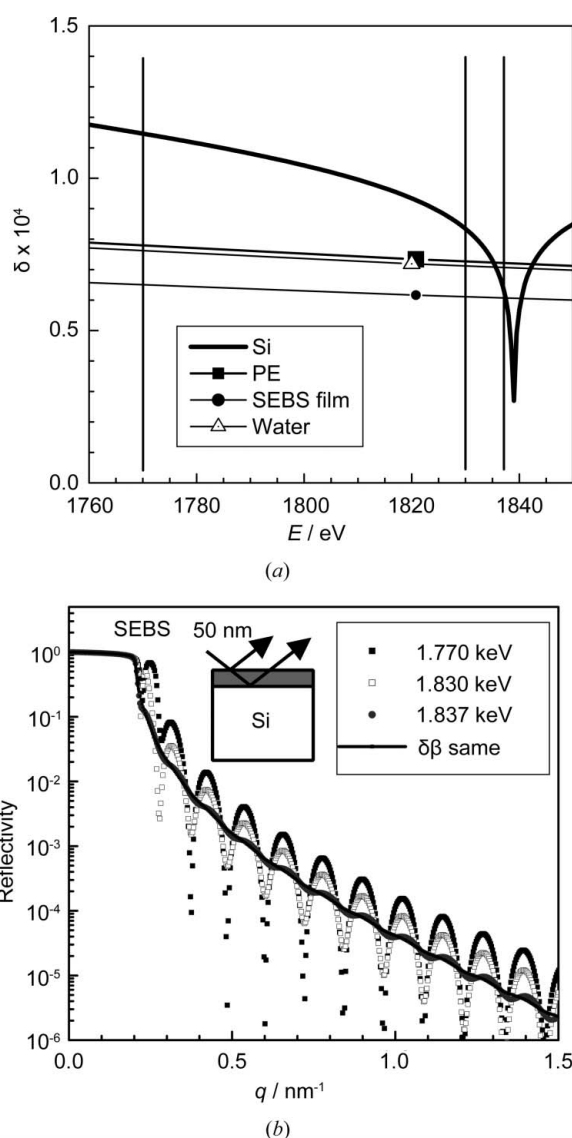


Figure 1
(a) The real parts of the refractive indices, δ , for an Si substrate, polystyrene (PS), SEBS films and water at the Si *K* absorption edge. They were calculated from reported values of the anomalous scattering factors and densities. For SEBS, the density of the present sample was determined from the critical angle measurements at Cu *K* α 1. (b) Reflectivity curves calculated for a model sample having 50 nm of SEBS film on an Si substrate. The refractive indices are taken from the above.

3. Results and discussion

Fig. 2(a) shows the GISAXS pattern for hard X-rays, observed with a photon energy of 12.4 keV and an incident angle of 0.15° . The profile obtained for the sample was characterized by a set of streaks elongated in the direction perpendicular to the substrate, with relatively sharp maxima in the in-plane direction. This suggests that the microphase separation structure of the thin film has a well defined in-plane order. The ratio of the magnitude of the in-plane scattering vector of the second streak to the first streak is 1.71 (3), in agreement with that for a two-dimensional hexagonal lattice. From depth-resolved GISAXS measurements at 1.770 keV (Okuda *et al.*, 2011), it was found that the structure of the micro phase separation in a thick SEBS film is relaxed within approximately 30–50 nm from the surface. This indicates that the thin film, which is strongly affected by both the substrate and the surface, might have a microstructure different from that of the bulk. Therefore, it is worthwhile to seek a method that avoids the complication caused by reflected beams from Si. The peak position in Fig. 2(a) yields an in-plane lattice parameter of 24.4 (3) nm, which agrees with the average spacing obtained from surface topography by a scanning probe microscope. Two horizontal lines are visible around $q_z = 0.25 \text{ nm}^{-1}$, which correspond to the lines representing the surface-enhanced scattering (the Yoneda line) and the reflected-refracted scattering at higher q_z .

The GISAXS patterns measured near the *K* absorption edge of Si are shown in Figs. 2(b) and 2(c). The angle of incidence was 0.75° for soft X-rays. At 1.770 keV, the scattering pattern near the Yoneda line is similar to that obtained at 12.4 keV, which means that the pattern

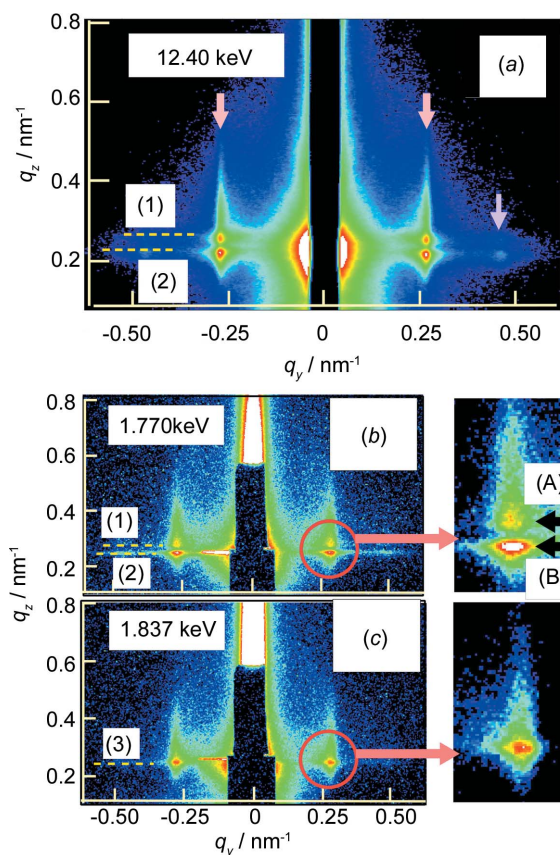


Figure 2
GISAXS patterns measured with X-rays with photon energies of (a) 12.4 keV, (b) 1.770 keV and (c) 1.837 keV. The positions marked by broken lines correspond to calculated (1) $k_i^z + k_c^z(\text{Si})$ and (2) $k_i^z + k_c^z(\text{SEBS})$ and (3) both.

reflects the scattering by both the incident and reflected beams. The two peaks shown in the encircled region of Fig. 2(b), and also by the arrows in the enlarged figure, are observed at 1.770 keV, and their positions in q_z almost agree with the calculated $k_i^z + k_c^z$ shown by the horizontal broken lines (1) and (2), where k_i^z is the z component of the incoming wave vector and $k_c^z(\text{Si})$ and $k_c^z(\text{SEBS})$ are the z components of the outgoing wave vector corresponding to the critical angles for Si and SEBS, respectively. In contrast, the peak marked (1) in Fig. 2(b) disappears at 1.837 keV, just below the absorption edge. From Fig. 1, the contrast of the real part of the refractive indices between the polymer and the Si substrate vanishes at 1.837 keV, because the refractive index of the substrate matches that of the film. Accordingly, the amplitude of the wave reflected at the polymer/Si interface becomes very small and the scattering invoked by the specularly reflected wave at the polymer/Si interface disappears. Eliminating such extra scattering is particularly useful when the microstructure of the film is less regular and quantitative analysis of the diffuse scattering near the Yoneda line is necessary. It is thus shown that anomalous dispersion at the Si K absorption edge is useful to control the contrast between the substrate and the polymer thin film, and even to eliminate the contrast between them. Although the photon flux in the present measurement is still low for a quantitative profile analysis, the approach makes it possible to obtain a GISAXS profile free from the effects of the strong reflection that occurs at the interface between the film and the substrate.

GISAXS measurements at the Photon Factory were performed under proposal 2010-G075, and those at SPring-8 were made as

proposal 2010-G075/ 2011A7297 with the permission of the BL03XU Frontier Soft-Materials Beamline Committee of SPring-8.

References

- Babonneau, D., Petroff, F., Maurice, J. L., Fettar, F., Vaures, A. & Naudon, A. (2000). *Appl. Phys. Lett.* **76**, 2892–2894.
- Busch, P., Rauscher, M., Smilgies, D.-M., Posselt, D. & Papadakis, C. M. (2006). *J. Appl. Cryst.* **39**, 433–442.
- Chantler, C. T. (1997). *NIST X-ray Form Factor, Attenuation and Scattering Tables*, <http://physics.NIST.gov/PhysRefData/FFast/html/form.html>.
- Ibel, K. & Stuhrmann, H. B. (1975). *J. Mol. Biol.* **93**, 255–265.
- Ishiji, K., Okuda, H., Hashizume, H., Almokhtal, M. & Hosoi, N. (2002). *Phys. Rev. B*, **66**, 014443.
- Lazzari, R. (2002). *J. Appl. Cryst.* **35**, 406–421.
- Lee, B., Park, I., Yoon, S., Park, S., Kim, J., Kim, K.-W., Chang, T. & Ree, M. (2005). *Macromolecules*, **38**, 4311–4323.
- Levine, J. R., Cohen, J. B., Chung, Y. W. & Georgopoulos, P. (1989). *J. Appl. Cryst.* **22**, 528–532.
- Masunaga, H. *et al.* (2011). *Polym. J.* **43**, 471–477.
- Okuda, H., Kato, M., Ochiai, S. & Kitajima, Y. (2009). *Appl. Phys. Express*, **2**, 126501.
- Okuda, H., Takeshita, K., Ochiai, S., Sakurai, S. & Kitajima, Y. (2011). *J. Appl. Cryst.* **44**, 380–384.
- Rauscher, M., Salditt, T. & Spohn, H. (1995). *Phys. Rev. B*, **52**, 16855–16863.
- Renaud, G., Lazzari, R. & Leroy, F. (2009). *Surf. Sci. Rep.* **64**, 225–380.
- Salditt, T., Li, C. & Spaar, A. (2006). *Biochem. Biophys. Acta*, **1758**, 1483–1498.
- Sinha, S. K., Sirota, E. B., Garoff, S. & Stanley, H. B. (1988). *Phys. Rev. B*, **38**, 2297–2311.
- Stuhrmann, H. B. (2007). *J. Appl. Cryst.* **40**, s23–s27.
- Tolan, M. (1999). *X-ray Scattering from Soft-Matter Thin Films*. Berlin: Springer Verlag.